



Published in final edited form as:

Angew Chem Int Ed Engl. 2021 November 02; 60(45): 24153–24161. doi:10.1002/anie.202108338.

Engineering fluorophore recycling in a fluorogenic RNA aptamer

Xing Li^a, Jiahui Wu^b, Samie R. Jaffrey^b

^aBeijing Institutes of Life Science, Chinese Academy of Sciences, Beijing, 100101, PR China; and Department of Pharmacology, Weill Cornell Medicine, Cornell University, New York, NY 10065 (USA)

^bDepartment of Pharmacology, Weill Cornell Medicine, Cornell University, New York, NY 10065 (USA)

Abstract

Fluorogenic aptamers can potentially show minimal photobleaching during continuous irradiation since any photobleached fluorophore can exchange with fluorescent dyes in the media. However, fluorophores have not been designed to maximize “fluorophore recycling.” Here we describe TBI, a novel fluorophore for the Broccoli fluorogenic aptamer. Previous fluorophores either fail to rapidly dissociate when they undergo photobleaching via *cis-trans* isomerization, or bind slowly, resulting in extended periods after dissociation of the photobleached fluorophore when no fluorophore is bound. By contrast, photobleached TBI dissociates rapidly from Broccoli, and TBI from the media rapidly replaces dissociated photobleached fluorophore. Using TBI, Broccoli exhibits markedly enhanced fluorescence in cells during continuous imaging. These data show that designing fluorophores to optimize fluorophore recycling can lead to enhanced fluorescence of fluorogenic aptamers.

Graphical Abstract

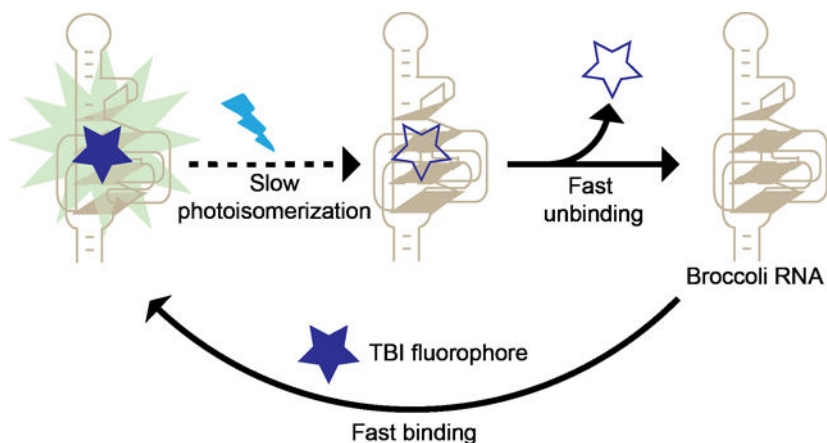
Fluorogenic RNA aptamers bind and activate the fluorescence of otherwise nonfluorescent dyes. Here we show an approach to maximize their fluorescence by reducing the impact of photobleaching. We engineered TBI, a fluorophore which rapidly dissociates upon photobleaching and can be rapidly replaced by TBI in the media. By maximizing “fluorophore recycling” we achieve higher fluorescence and enable long-term fluorescence imaging.

lix@biols.ac.cn, srj2003@med.cornell.edu.

Conflict of interest

S.R.J. is the co-founder of Lucerna Technologies and has equity in this company. Lucerna has licensed technology related to Spinach and other RNA-fluorophore complexes.

Supporting information for this article is given via a link at the end of the document.



Keywords

RNA imaging; Fluorophore recycling; Photostability; Fluorescent probes

Introduction

A unique feature of fluorogenic aptamers, compared to fluorescent proteins, is that fluorogenic aptamers noncovalently and reversibly bind their cognate fluorophore.^[1] As a result, the bound fluorophore can unbind and exchange with fluorophore in solution. This is advantageous compared to fluorescent proteins, which contain an integral fluorophore. Once the fluorophore is photobleached, the fluorescent protein is permanently nonfluorescent.^[1a] Thus, fluorogenic aptamers are different from proteins since they can exhibit long-lived fluorescence due to “fluorophore recycling,” i.e., continuous exchange of bound fluorophores, which restores fluorescence if a fluorophore becomes photobleached.^[3–4]

For optimal fluorophore recycling, the aptamer should have a bound non-photobleached fluorophore for as much time as possible. This will not occur if the time between unbinding of a fluorophore and rebinding of a new fluorophore is long. Additionally, if the photobleached fluorophore does not unbind quickly, the aptamer will have reduced fluorescent output. Thus the kinetics of binding of a fresh fluorophore and unbinding of the photobleached fluorophore are essential parameters that determine the fluorescence output of a fluorogenic aptamer.

Fluorophore recycling has been characterized with the Spinach aptamer^[1a, 4–5] and the Broccoli aptamer, which has a highly similar DFHBI fluorophore-binding pocket.^[1f, 1k, 3, 6] Under low light conditions, DFHBI undergoes efficient fluorophore recycling, and the resulting Spinach-DFHBI complex remains fluorescent for more than 2500 sec.^[1a] However, with higher light intensities, Spinach and Broccoli exhibit marked reductions in fluorescence output due to inefficient fluorophore recycling.^[1f] The poor fluorophore recycling is caused by two distinct problems with DFHBI. First, the *trans*- form of DFHBI that forms due to photoisomerization^[3–5] exhibits slow dissociation from the aptamer.^[3] Second, the rebinding rate of *cis*-DFHBI from the media is relatively slow ($k_{on} = 81,000 \text{ M}^{-1} \text{ sec}^{-1}$).^[5] The first problem was resolved recently with a new fluorophore, BI (3,5-difluoro-4-

hydroxybenzylidene imidazolinone –1-benzimidazole), a DFHBI derivative with an added benzimidazole substituent.^[3] The isomerized *trans*-BI molecule, unlike *trans*-DFHBI, cannot be accommodated by the aptamer and thus rapidly dissociates.^[3]

Although the slow unbinding rate of *trans*-DFHBI was resolved by using BI, the binding rate (k_{on}) of BI remains relatively slow ($k_{\text{on}} = 13,600 \text{ M}^{-1} \text{ sec}^{-1}$).^[3] The slow on-rate can result in long periods of time during which no fluorophore is bound to Broccoli, thus leading to reduced overall fluorescence output. It remains unclear if enhancing fluorophore recycling by increasing the binding rate would result in improved fluorescence output and the appearance of greater photostability.

Here we used a structure-guided strategy to generate a TBI (3,5-difluoro-4-hydroxybenzylidene-2-thioximidazolidin-1-benzimidazole), a DFHBI-related fluorophore with an increased on-rate. This increase in on-rate leads to enhanced fluorophore recycling, which correlates with increased brightness and photostability of Broccoli-TBI compared to previous fluorophores. These results show how controlling the binding and unbinding rates of the fluorophore can result in RNA-fluorophore complexes with optimized fluorescence properties.

Results and Discussion

Rational Design of DFNS

Unlike conventional small molecule fluorescent dyes which can undergo photobleaching by undergoing irreversible chemical modification, photobleaching of Spinach-DFHBI is mediated by a *cis-trans* photoisomerization of DFHBI.^[4–5] Spinach exhibits low fluorescence when bound to *trans*-DFHBI. Next, *trans*-DFHBI unbinds. Lastly, a *cis*-DFHBI fluorophore from solution binds to Broccoli, which restores fluorescence (Scheme 1). Spinach and Broccoli, when bound to DFHBI, show fast photobleaching, and slow fluorescence recovery^[4–5], which ultimately limits fluorescence output. The rapid photobleaching is due to rapid *cis-trans* isomerization^[4], and the slow recovery is due to slow dissociation of the *trans*-DFHBI isomer and slow rebinding of *cis*-DFHBI from solution.^[3–5]

To increase photostability, we previously developed BI, a DFHBI derivative.^[1k, 3, 7] BI improves photostability since it shows reduced *cis-trans* isomerization (Scheme S1). BI also improves fluorophore recycling since BI exhibits rapid dissociation when it forms the *trans*-BI isomer (Scheme S1).^[3] BI shows these improvements relative to DFHBI since BI contains a benzimidazole which was predicted to make additional contacts with the RNA aptamer. These contacts suppress *cis-trans* isomerization.^[3] The rapid dissociation of *trans*-BI was due to the inability of the *trans*-BI to be accommodated within the fluorophore-binding pocket of Broccoli.^[3] Thus, BI exhibits reduced photobleaching and improves one aspect of fluorophore recycling.

Although Broccoli-BI complexes were markedly more photostable, the steady-state fluorescence was substantially lower than the initial cellular fluorescence (Figure 4B and 4C). The steady-state fluorescence reflects the balance between light-induced fluorophore

dissociation and rebinding of fluorophore. Since the rebinding rate of BI is relatively slow ($13,600 \text{ M}^{-1} \text{ s}^{-1}$)^[3], we reasoned that a fluorophore with increased rebinding ability would show enhanced fluorophore recycling and thus improved fluorescence.

To address this, we asked if we could modify the DFHBI core to increase the binding rate. Several studies have shown that methyl substituents can adversely affect binding rates for a variety of small molecules that interact with proteins.^[8] The methyl moiety of DFHBI binds in a relatively small pocket within the RNA as seen in the Spinach-DFHBI crystal structure (Figure 1A). We therefore considered the possibility that DFHBI derivatives containing substituents at the C2 position that are smaller than a methyl moiety (Figure 1B) might show increased binding rates.

We therefore synthesized a series of DFHBI derivatives with smaller substituents on the C2 position in place of the methyl. We thus synthesized DFHBI derivatives with heteroatom substitutions at the C2 and N3 positions (Figure 1B).

In the case of the N3 position, we substituted the imine with sulfur, forming a methanedithioate (DFSS) (Figure 1B). We also converted the imine to a thioester (DFNS), which results in a ketone in place of the C2 methyl. Lastly, we synthesized DFNM ((Z)-2-(4-(3,5-difluoro-4-hydroxybenzylidene)-1-methyl-5-oxoimidazolidin-2-ylidene)malononitrile), in which the methyl was replaced with a dicyanoethane. Although the cyanoethane is larger than a methyl substituent, the shorter ethylene bond may be sufficient to improve binding.

We first measured the absorption of these derivatives (20 μM) in solution. Compared to DFHBI-1T ((Z)-4-(3,5-difluoro-4-hydroxybenzylidene)-2-methyl-1-(2,2,2-trifluoroethyl)-1H-imidazol-5(4H)-one), DFNS, DFSS, DFNM exhibited a $\sim 5 \text{ nm}$, 20 nm, 100 nm red-shifted absorption, respectively (Figure S1).

We next asked if these derivatives exhibit red-shifted absorbance and emission spectra compared to DFHBI-1T when bound to Broccoli. To ensure that each Broccoli aptamer was bound to fluorophore, each derivative (0.5 μM) was tested at a concentration that was 50X the concentration of Broccoli (10 μM). As with the absorbance, each derivative (0.5 μM) showed substantially red-shifted excitation and emission peaks relative to DFHBI-1T (Figure 1C, Figure S1, Table S1).

Additionally, we measured the fold-enhancement of fluorescence of each derivative (0.5 μM) upon binding Broccoli (10 μM). All compounds showed low levels of Broccoli-induced fluorescence except for DFNS (Figure S2). Additionally, Broccoli-DFNS shows a 10% increase in the extinction coefficient relative to Broccoli-DFHBI-1T (Table 1). Based on this, DFNS appeared particularly promising for subsequent analysis.

A requirement for any fluorophore used by a fluorogenic aptamer is that it should show low background fluorescence activation by cellular components. To test the derivatives, HEK293T cells were pretreated for 1 h with each derivative or DFHBI-1T (10 μM), which we previously found to exhibit extremely low fluorescence in cells.^[9] Comparison of the different fluorophores showed that DFNS shows a low background fluorescence that was

slightly higher than DFHBI-1T, indicating that DFNS did not show substantial nonspecific fluorescence activation by cellular components. However, the background fluorescence of DFSS and DFNM was significantly higher than DFHBI-1T (Figure S3). Thus, these compounds were not further examined for in-cell experiments.

We next asked if DFNS (10 μM) exhibits fluorescence activation by Broccoli expressed in HEK293T cells. In these experiments, Broccoli was highly expressed as a circular RNA using the Tornado expression system.^[10] In these experiments, we observed green fluorescence only in Broccoli-expressing cells, but not control transfected cells. Notably, the fluorescence was ~50% higher than the fluorescence levels than DFHBI-1T-treated cells (Figure 1D, S4). Based on these *in vitro* and *in vivo* experiments, DFNS shows improved brightness relative to DFHBI-1T.

We next asked if the increased brightness of DFNS-Broccoli complexes reflects increased photostability in cells. Photobleaching is caused by *cis-trans* isomerization of the Broccoli-bound fluorophore, and can be detected by measuring the drop in cellular fluorescence after irradiating cells.^[3] The initial slope of the drop in fluorescence reflects the rate of isomerization from *cis* to *trans*.^[3-4] We measured total cellular fluorescence during continuous irradiation over 30 s in an epifluorescence microscope (Figure 1D and 1E). In these experiments, DFNS or DFHBI-1T (10 μM) were preincubated with cells for 1 h and the fluorescence in a selected region of interest in the cytosol of a minimum of three cells was measured. As expected, the fluorescence in DFHBI-1T-treated HEK293 cells expressing circular Broccoli showed rapid loss of fluorescence. A very similar initial drop in fluorescence was seen in DFNS-treated cells (Figure 1D and 1E). This suggests that the overall photostability was not changed with DFNS compared to DFHBI-1T.

We next asked if DFNS showed improved fluorophore recycling. During a photobleaching experiment, the fluorescence does not go to zero. Instead, the fluorescence reaches a plateau which reflects fluorophore recycling, i.e., an equilibrium between unbinding of the photobleached (i.e. *trans* form) fluorophore and the rebinding of *cis*-form from solution.^[3] Indeed, we observed that Broccoli-expressing cells treated with DFNS exhibit a much higher plateau compared to DFHBI-1T (Figure 1E).

We also tested photostability and fluorophore recycling *in vitro*. To test this, we incubated 100 μL of Broccoli (10 μM) and DFNS or DFHBI-1T (1 μM). In these experiments, a 100 μl sample was quantified in cuvette in a fluorimeter. As with the experiments in cells, the photobleaching rate, as measured by the initial slope of the fluorescence loss, was similar with both DFNS and DFHBI-1T. Additionally, as with the cell-based experiments, fluorophore recycling appeared more efficient with DFNS as Broccoli-DFNS based on the substantially higher plateau with DFNS (Figure 1F). It is important to note that the observed photobleaching rate *in vitro* is much slower than the rate observed in cells (see Figure 1E) due to the lower light intensity used in the *in vitro* experiments. Overall, these experiments suggest that DFNS undergoes substantially improved fluorophore recycling compared to DFHBI-1T.

DFNS exhibits rapid binding of *cis*-form and unbinding of *trans*-form

The increased fluorophore recycling of DFNS compared to DFHBI-1T can be caused by increased unbinding rate (k_{off}) of the photobleached *trans*-DFNS or increased binding rate (k_{on}) of fresh *cis*-DFNS from the media. We therefore first measured k_{on} . To measure k_{on} , RNA is added to the fluorophore, resulting in a monoexponential increase in fluorescence signal, giving the observed rate constant (k_{obs}). The slope of the linear fit of the k_{obs} plot provides k_{on} .^[4] We observed the k_{on} of DFNS is ~14 times higher than k_{on} of DFHBI-1T (Figure 2A and 2B). Thus, a higher DFNS binding rate may contribute to the increased fluorophore recycling of DFNS.

An improvement in k_{on} would increase fluorophore recycling only if k_{on} , rather than k_{off} , is rate limiting. However, k_{off} cannot be easily measured since the fluorophore cannot be synthesized in a pure photobleached *trans*- form. The fluorophores are in a *cis-trans* equilibrium, with the *cis* form being the most thermodynamically favorable.^[4] Thus, to determine if k_{off} or k_{on} is rate limiting, we used a different approach. As described previously^[3], we irradiate Broccoli-fluorophore complexes in cells to induce formation of the *trans*-fluorophore. At very low fluorophore concentrations, when k_{on} is low, k_{on} will be rate limiting. However, as the k_{on} is increased, there will be a point where there is no increase in fluorescence—this occurs once k_{off} is less than the product of k_{on} and the fluorophore concentration, and thus k_{off} becomes rate limiting. Therefore, the concentration of fluorophore at which there is no more increase in the fluorescence plateau indicates the point at which k_{off} becomes rate limiting.^[3]

We therefore measured the fluorescence of Broccoli in HEK293T cells cultured with increasing concentrations of fluorophore to increase the rate of fluorophore binding to Broccoli (Figure 2B). The cytoplasm of selected cells was imaged using continuous illumination, resulting in a drop in the cellular fluorescence until the plateau was reached. When we tested increasing concentrations of DFNS, we observed an increase in the fluorescence plateau with increasing concentrations of DFNS (Figure 2A and 2C). This indicates that k_{on} is rate limiting under all conditions tested. In contrast, we did not see a change in the plateau with increasing concentrations of DFHBI-1T, indicating that k_{off} is rate limiting for this fluorophore (Figure 2A and 2B). In summary, DFNS and DFHBI-1T are fundamentally different: the *trans*-DFNS fluorophore unbinds rapidly, allowing a rapid restoration of fluorescence upon rebinding of *cis*-DFNS. In contrast, the unbinding of the *trans*-DFHBI-1T is slow, and therefore the cytoplasm of selected cells was increasing the DFHBI-1T concentration, and thus its binding rate, does not affect cellular fluorescence. Overall, these data show that *trans*-DFNS undergoes rapid unbinding, which then allows fluorescence to be restored when a new fluorophore binds the Broccoli.

Design and synthesis of TBI by combining BI and DFNS

A major feature of BI is that it shows resistance to light-induced *cis-trans* isomerization. This effect is due to its additional contacts with Broccoli. Despite this advantageous property, BI shows a relatively slow k_{on} ($13,600 \text{ M}^{-1} \text{ s}^{-1}$), similar to the k_{on} of DFHBI-1T ($14,900 \text{ M}^{-1} \text{ s}^{-1}$).^[3] Thus, BI has good resistance to photoisomerization but poor k_{on} , while DFNS is highly susceptible to photoisomerization, but has desirable k_{on} and k_{off} . We

therefore attempted to design a fluorophore which would have the desirable properties of both DFNS and BI (Figure 3A).

To merge the properties of BI and DFNS, we designed TBI (3,5-difluoro-4-hydroxybenzylidene-2-thioxoimidazolidin-1-benzoimidazole). TBI contains the benzimidazole moiety of BI, which accounts for the high affinity binding of BI and the rapid k_{off} of trans-BI.^[3] TBI also contains the smaller thioester substituent on the C2 position, which appears to mediate its improved k_{on} . We first assessed the spectral properties of TBI (0.5 μM) in the presence and absence of Broccoli (10 μM). TBI exhibited a similar emission as DFNS, but also a ~ 15 nm red-shifted excitation when bound to Broccoli compared to DFNS (Figure 3B and Table 1).

TBI exhibits the main properties needed for imaging Broccoli. First, TBI exhibits a more than 13,000-fold fluorescent enhancement when bound to Broccoli (Figure 3C). In these experiments, the fluorescence of TBI (0.5 μM) was measured in the absence and presence of Broccoli (10 μM). TBI showed low fluorescence in the absence of Broccoli, and high quantum yield (0.644) when bound to Broccoli (Figure 3C, Table 1). The brightness is similar to BI, and more than 3 times higher than DFNS (Table 1). The Broccoli-TBI complex showed maximal fluorescence at pH 7.5, with decreased fluorescence at lower pH (Figure. S5).

TBI also exhibits a similarly high binding affinity as BI with Broccoli. To test this, we titrated the fluorophore and measured fluorescence to extrapolate the dissociation constant (K_{D}). Like BI ($K_{\text{D}} = 51$ nM), TBI ($K_{\text{D}} = 71$ nM) exhibits ~ 9 times higher in binding affinity compared to DFNS ($K_{\text{D}} = 646$ nM) (Table 1). The binding affinity data suggest that the benzimidazole in TBI provides additional contacts with Broccoli that confer increased binding affinity.

We next examined background fluorescence and Broccoli-induced fluorescence of TBI (10 μM) in HEK293T cells. TBI showed similar intrinsic background fluorescence as DFNS (10 μM) in HEK293T cells (Figure 3C). After adding either TBI or BI, we observed similar cellular fluorescence levels (Figure 3D), which was ~ 10 times higher than DFNS-treated cells. Based on these experiments, TBI possesses the same ability to stabilize the folded state of Broccoli that is seen with BI. Overall, TBI shows low cellular background, high Broccoli-induced fluorescence in vitro, and high cellular fluorescence in cells.

Broccoli-TBI exhibits both enhanced fluorophore recycling and increased photostability

We next asked if Broccoli-TBI exhibits increased photostability and fluorophore recycling. First, we tested photostability in cells. As before, we measured total cellular fluorescence during continuous irradiation over 30 s in an epifluorescence microscope. In these experiments, fluorophores (10 μM) were preincubated with cells for 1 h and the fluorescence in a selected region of interest in the cytosol of a minimum of three cells was measured. Here, we observed that the initial drop in fluorescence of Broccoli-TBI was similar to Broccoli- BI, and ~ 3 times slower than Broccoli-DFNS (Figure 4A and 4B). Thus, TBI shows increased photostability.

Similar effects were seen in vitro, using cuvette-based irradiation of Broccoli (1 μM) and fluorophore (0.1 μM) (Figure 4C).

We next asked if TBI shows enhanced fluorophore recycling. For these experiments, we measured the fluorescence plateau in Broccoli-expressing cells and in vitro. We found that all three fluorophores achieved the plateau in fluorescence at 30 sec in cells using irradiation from the epifluorescence microscope, and in 10 min with a fluorimeter. In each case, TBI showed the highest plateau (Figure 4B and 4C).

Importantly, the k_{on} of TBI is ~ 5 times higher than k_{on} of BI (Figure S6). Thus, TBI is an improvement over BI with respect to fluorophore recycling. However, the k_{on} of TBI is not as fast as DFNS, most likely because TBI contains a bulky benzimidazole substituent at N1 position. Nevertheless, the benzimidazole substituent is beneficial since it markedly increases k_{off} after photoisomerization since the *trans* form of the fluorophore cannot be accommodated in the fluorophore-binding pocket of Broccoli.^[3] Overall, TBI is an improvement relative to BI due to its higher k_{on} .

We next asked if TBI improves long-term cellular imaging of Broccoli. Long-term imaging is achieved by acquiring images periodically, and then closing the shutter to prevent irradiation of the sample.^[4] During this recovery time period, fluorophore recycling can occur to allow fluorescence to recover. In this way, Broccoli can be imaged for long time periods without the normal limitations that come from photobleaching. For these experiments, we imaged circular Broccoli fluorescence in HEK293 cells over 250 s. Images (500 ms) were acquired with 10 s recovery periods.

We first imaged circular Broccoli using BI. Here we observed fluorescence recovery during the 10 s recovery period, although the recovery was clearly not complete (Figure 4D). In contrast, cells treated with TBI exhibited a significantly greater recovery of cellular fluorescence (Figure 4D). Overall, these data support the idea that TBI exhibits a higher fluorophore recycling, enabling more efficient long-term imaging of Broccoli.

Overall these experiments show that TBI enhances the imaging of Broccoli in mammalian cells, which is most evident during long-term imaging experiments.

Conclusion

Although there are now a large number of fluorogenic aptamers, there is little insight into how to overcome photobleaching, which is an inevitable process for nearly all fluorescent molecules. In this study, we show that the loss of fluorescence caused by photobleaching can be overcome by rationally designing a fluorophore that undergoes rapid recycling after photobleaching. Our approach takes advantage of the photobleaching mechanism of DFHBI-related fluorophores, which involves light-induced *cis* to *trans* isomerization. We developed TBI, a fluorophore which rapidly unbinds from the Broccoli aptamer once it is photoisomerized to the low-fluorescence *trans* form, and then can be rapidly replaced by *cis*-TBI from the media. Overall, these data show that fluorophore recycling can be used to rapidly replace photoisomerized fluorophores and thus maximize the time that Broccoli is capable of producing fluorescence.

To develop TBI, three main features were optimized: photoisomerization rate, k_{off} of the *trans* form of TBI, and k_{on} of the *cis* form of TBI. To minimize photoisomerization, TBI relied on the key structural feature of BI: a benzimidazole attached to the N1 position of DFHBI. We previously showed that the benzimidazole suppresses *cis-trans* isomerization by creating additional attachment points for the fluorophore to bind Broccoli.^[3] The benzimidazole also ensures a high k_{off} , since the *trans* form of the fluorophore cannot fit within the ligand-binding pocket of Broccoli.^[3] However, BI has a relatively slow k_{on} , which prevents rapid replacement of the *trans* fluorophore.

To maximize the k_{on} , we replaced a methyl substituent on the C2 carbon on DFHBI with a thione. This substitution caused a 14-fold increase in k_{on} , presumably reflecting that the smaller size of the thione compared to the methyl moiety. The methyl moiety binds within a relatively small space facing the C2 carbon in Broccoli (Figure 1A). The smaller thione moiety may be accommodated more readily, accounting for the increased k_{on} . By adding this feature to BI, we created TBI, a fluorophore in which all three of these critical features have been optimized.

In principle it is possible to increase the k_{on} by simply increasing the concentration of the fluorophore since the overall on rate is proportional to k_{on} and the concentration of the fluorophore. However, at concentrations of fluorophore above 10 μM , DFHBI-related fluorophores start to show nonspecific fluorescence activation in cells.^[1f, 3] Therefore, the k_{on} has to be optimized using a fluorophore concentration of 10 μM or less.

Our findings highlight how the photobleaching mechanism of a fluorophore should be considered when developing novel fluorogenic aptamer-fluorophore pairs. In the case of DFHBI-related fluorophores, the fluorophore undergoes *cis-trans* isomerization. The large conformational change associated with isomerization can be exploited to achieve highly efficient unbinding, as has been seen with BI^[3] and TBI. However, fluorophores of other classes may undergo photobleaching through other mechanisms, such as oxidation^[11] or through entry into triplet states.^[12] If the conformation of the fluorophore does not change, then the non-fluorescent form will stay bound.

The recycling rate depends on the off-rate of the photobleached fluorophore, which may be very slow for high-affinity fluorophores that do not undergo large conformational changes upon photobleaching. Thus, for these high affinity fluorophores, fluorophore recycling can be impaired because the fluorogenic aptamer will retain the non-fluorescent fluorophore for a long period of time, thus reducing the overall fluorescence output. In contrast, fluorophores such as BI and TBI that undergo conformational changes upon photobleaching can be highly advantageous since the conformational change can dramatically increase the off-rate.

Paradoxically, some fluorophores may be improved if their affinity is reduced. A reduced affinity can be caused by relatively rapid unbinding rates, regardless of whether the fluorophore is photobleached or not. If the fluorophore also has a rapid on rate, then the fluorophore will be constantly recycling, which would maintain the aptamer-fluorophore complex in a fluorescent form.

Using TBI, Broccoli can be imaged for extended periods with minimal loss in fluorescence. This can allow longer continuous imaging experiments of Broccoli-labeled RNA, and can improve the ability to quantify Broccoli-tagged RNAs and Broccoli-based sensor-derived fluorescence. Broccoli-TBI may have ideal properties for super-resolution microscopy techniques that rely on fluctuating fluorescence emissions from bright to dark states. The ability of TBI to produce greater fluorescence before photobleaching, compared to DFHBI, along with the rapid restoration of fluorescence due to improve k_{on} may allow sufficient blinking for super resolution imaging.^[13]

As other fluorogenic aptamers are designed, the overall design principles described here may enable further improvement and optimization of fluorescence output.

Supplementary Material

Refer to Web version on PubMed Central for supplementary material.

Acknowledgements

We thank T. Hagen, Q. Hou, W. Zhan, and Y. Huang for their useful help and comments. This work was supported by Talent research start-up fund, Beijing Institutes of Life Science, Chinese Academy of Sciences (CAS), NIH grant R35 NS111631 (S.R.J.) and Starr Cancer Consortium Grant I12-0051(S.R.J.).

References

- [1]. a)Paige JS, Wu KY, Jaffrey SR, Science 2011, 333, 642–646; [PubMed: 21798953] b)Paige JS, Nguyen-Duc T, Song W, Jaffrey SR, Science 2012, 335, 1194–1194; [PubMed: 22403384] c)Hoshika S, Leal NA, Kim M-J, Kim M-S, Karalkar NB, Kim H-J, Bates AM, Watkins NE, SantaLucia HA, Meyer AJ, DasGupta S, Piccirilli JA, Ellington AD, SantaLucia J, Georgiadis MM, Benner SA, Science 2019, 363, 884–887; [PubMed: 30792304] d)Jung JK, Alam KK, Verosloff MS, Capdevila DA, Desmau M, Clauer PR, Lee JW, Nguyen PQ, Pastén PA, Matiassek SJ, Gaillard J-F, Giedroc DP, Collins JJ, Lucks JB, Nat. Biotechnol 2020;e)Dolgosheina EV, Jeng SC, Panchapakesan SSS, Cojocar R, Chen PS, Wilson PD, Hawkins N, Wiggins PA, Unrau PJ, ACS Chem. Biol 2014, 9, 2412–2420; [PubMed: 25101481] f)Song W, Filonov GS, Kim H, Hirsch M, Li X, Moon JD, Jaffrey SR, Nat. Chem. Biol 2017, 13, 1187–1194; [PubMed: 28945233] g)Chen X, Zhang D, Su N, Bao B, Xie X, Zuo F, Yang L, Wang H, Jiang L, Lin Q, Fang M, Li N, Hua X, Chen Z, Bao C, Xu J, Du W, Zhang L, Zhao Y, Zhu L, Loscalzo J, Yang Y, Nat. Biotechnol 2019, 37, 1287–1293; [PubMed: 31548726] h)Sunbul M, Jäschke A, Nucleic Acids Res. 2018, 46, e110–e110; [PubMed: 29931157] i)Bouhedda F, Fam KT, Collot M, Autour A, Marzi S, Klymchenko A, Ryckelynck M, Nat. Chem. Biol 2019;j)Li X, Mo L, Litke JL, Dey SK, Suter SR, Jaffrey SR, J. Am. Chem. Soc 2020, 142, 14117–14124; [PubMed: 32698574] k)Moon JD, Wu J, Dey SK, Litke JL, Li X, Kim H, Jaffrey SR, Cell Chem. Biol 2021;l)Ma K, Li X, Xu B, Tian W, Anal. Chim. Acta 2021, 338859. [PubMed: 34794573]
- [2]. Warner KD, Chen MC, Song W, Strack RL, Thorn A, Jaffrey SR, Ferre-D'Amare AR, Nat. Struct. Mol. Biol 2014, 21, 658–663. [PubMed: 25026079]
- [3]. Li X, Kim H, Litke JL, Wu J, Jaffrey SR, Angew. Chem., Int. Ed 2020, 59, 4511–4518.
- [4]. Han KY, Leslie BJ, Fei J, Zhang J, Ha T, J. Am. Chem. Soc 2013, 135, 19033–19038. [PubMed: 24286188]
- [5]. Wang P, Querard J, Maurin S, Nath SS, Le Saux T, Gautier A, Jullien L, Chemical Science 2013, 4, 2865–2873.
- [6]. Filonov GS, Song W, Jaffrey SR, Biochemistry 2019, 58, 1560–1564. [PubMed: 30838859]
- [7]. Wu J, Jaffrey SR, Curr. Opin. Chem. Biol 2020, 57, 177–183. [PubMed: 32829251]
- [8]. a)Leung CS, Leung SSF, Tirado-Rives J, Jorgensen WL, J. Med. Chem 2012, 55, 4489–4500; [PubMed: 22500930] b)Clackson T, Yang W, Rozamus LW, Hatada M, Amara JF, Rollins CT,

Stevenson LF, Magari SR, Wood SA, Courage NL, Lu X, Cerasoli F, Gilman M, Holt DA, Proc. Natl. Acad. Sci 1998, 95, 10437–10442; [PubMed: 9724721] c)Verhoeven MA, Bovee-Geurts PHM, de Groot HJM, Lugtenburg J, DeGrip WJ, J. Mol. Biol 2006, 363, 98–113. [PubMed: 16962138]

- [9]. Song W, Strack RL, Svensen N, Jaffrey SR, J. Am. Chem. Soc 2014, 136, 1198–1201. [PubMed: 24393009]
- [10]. Litke JL, Jaffrey SR, Nat. Biotechnol 2019, 37, 667–675. [PubMed: 30962542]
- [11]. Tasso TT, Schlothauer JC, Junqueira HC, Matias TA, Araki K, Liandra-Salvador E, Antonio FC, Homem-de-Mello P, Baptista MS, J. Am. Chem. Soc 2019, 141, 15547–15556. [PubMed: 31490678]
- [12]. Altman RB, Terry DS, Zhou Z, Zheng Q, Geggier P, Kolster RA, Zhao Y, Javitch JA, Warren JD, Blanchard SC, Nat. Meth 2012, 9, 68–71.
- [13]. a)Krishnan Y, Zou J, Jani MS, ACS Cent. Sci 2020, 6, 1938–1954; [PubMed: 33274271]
b)Chakraborty K, Veetil AT, Jaffrey SR, Krishnan Y, Annu. Rev. Biochem 2016, 85, 349–373. [PubMed: 27294440]

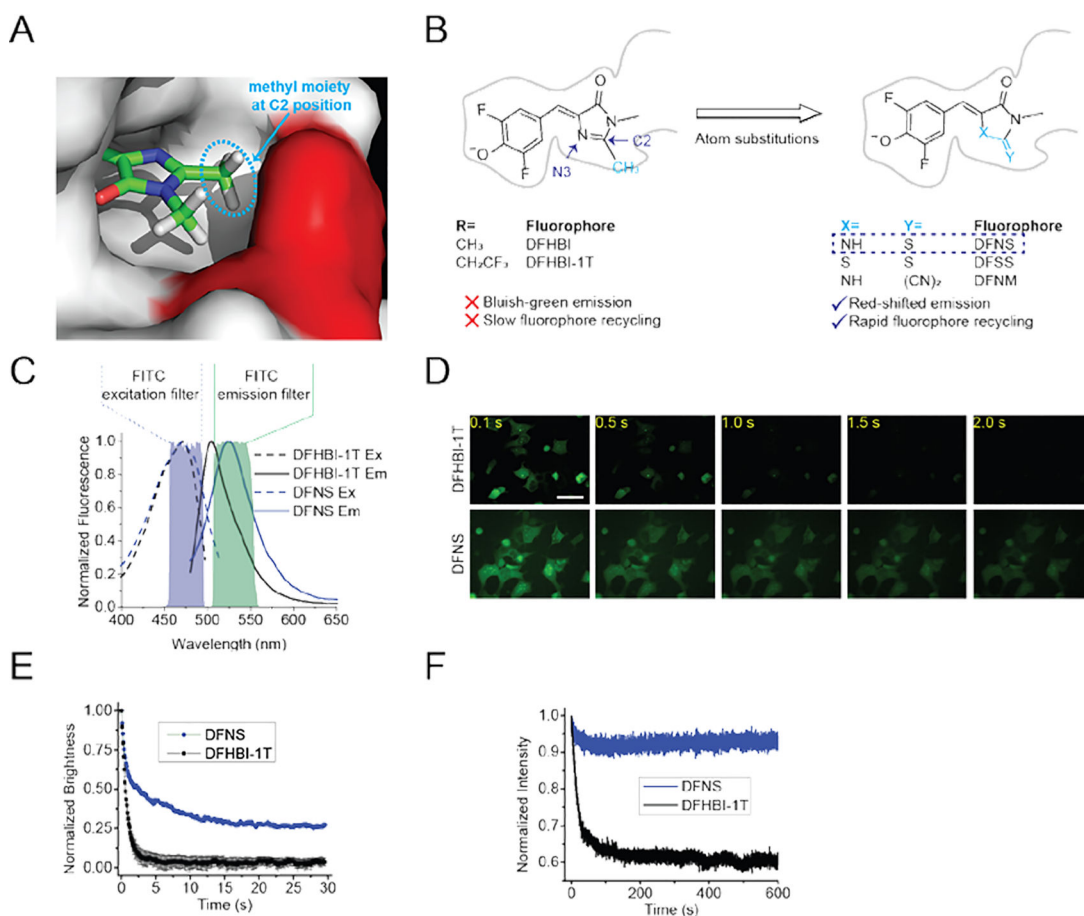


Figure 1. Identification of DFNS, a novel fluorophore with markedly increased recycling in Broccoli-expressing mammalian cells.

(A) The methyl moiety (indicated in a light blue dotted ellipse) at the C2 position of DFHBI binds in a relatively narrow groove in the RNA. Shown is the orientation of DFHBI in Spinach/Broccoli RNA based on the crystal structure.^[2] The methyl group on the C2 position closely abuts the A44 in Spinach (red). (B) Chemical structure of Broccoli-binding fluorophores, including DFHBI and DFHBI-1T as well as the fluorophores with atomic substitutions. To avoid having a methyl moiety (blue) at the C2 position, we synthesized three new fluorophores with less bulky substituents: DFNS, DFSS, DFNM. Compared to DFHBI-1T, DFNS exhibits the most red-shifted spectra (Figure 1C). DFNS also shows increased photostability, which reflects enhanced fluorophore recycling (see Figure 1D and 1E). (C) Fluorescence spectra of Broccoli-DFNS. Excitation (Ex, dotted line) and emission (Em, solid line) spectra were measured using 10 μ M Broccoli and 0.5 μ M DFNS or DFHBI-1T in buffer containing 40 mM HEPES pH 7.4, 100 mM KCl and 1 mM MgCl₂. Shown are the excitation and emission filters for the common FITC filter cubes. (D) and (E) DFNS shows improved fluorophore recycling in living cells compared to DFHBI-1T. *In vivo* photostability of Broccoli-fluorophore complexes (final concentration of 10 μ M for each fluorophore in the culture media) was assessed by continuous imaging of HEK293 cells expressing circular Broccoli. Images were acquired (100 ms/frame) using a 40 \times objective with a FITC filter cube. Scale bar, 50 μ m.

(E) Quantification of Broccoli-fluorophore photostability in HEK293 cells. The average brightness of Broccoli-expressing cells incubated with 10 μM DFHBI-1T or was DFNS was measured ($n = 3$ cells per measurement). DFHBI-1T and DFNS show a similar initial drop in fluorescence (between 0–0.5 sec). However, DFNS shows a higher plateau, indicating improved fluorophore recycling compared to DFHBI-1T. (F) Broccoli-DFNS exhibits higher photostability compared to Broccoli-DFHBI-1T *in vitro*. Fluorescence was measured in a solution containing 0.1 μM DFNS or DFHBI-1T and 1 μM Broccoli. The plot for DFHBI-1T is taken from ref. 3

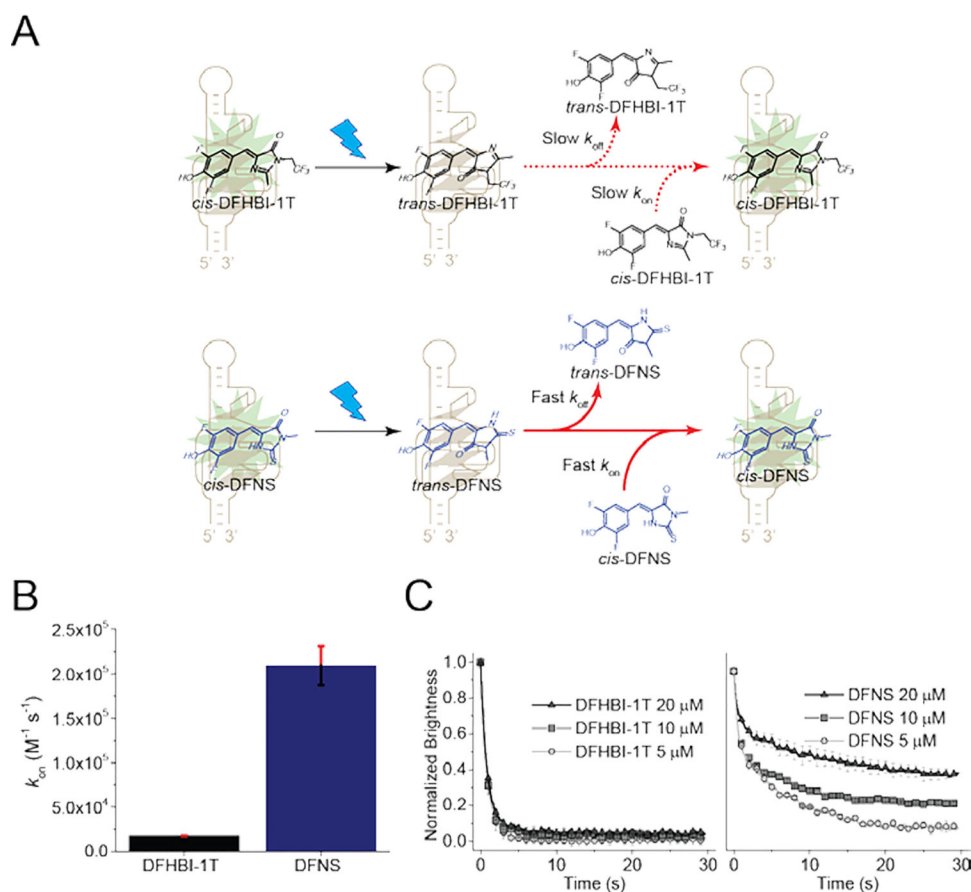


Figure 2. DFNS exhibits efficient fluorophore recycling.

(A) Schematic of *cis-trans* photoisomerization of Broccoli and the resoration of fluorescence by fluorophore recycling. Both DFHBI-1T (top) and DFNS (bottom) undergo *cis-trans* photoisomerization. Unlike DFHBI-1T, DFNS exhibits fast unbinding of the photobleached *trans* form and fast rebinding of the *cis* form. (B) DFNS exhibits markedly higher k_{on} compared to DFHBI-1T ($k_{on}=14,900 M^{-1} s^{-1}$ for DFHBI-1T; $k_{on}=209,200 M^{-1} s^{-1}$ for DFNS). (C) DFNS exhibits a higher k_{off} compared to DFHBI-1T. After photoisomerization of DFHBI fluorophores from *cis* to *trans*, fluorescence can only be restored once the *trans*-fluorophore unbinds from the RNA. If *trans*-fluorophore unbinding is slow, this step can be the rate limiting step in restoring fluorescence. To determine if *trans*-fluorophore unbinding is the rate limiting step, we measured photobleaching during continuous illumination of circular Broccoli-expressing HEK293T cells. Fluorescence diminishes over time and reaches a plateau. If unbinding is fast, then the rate-limiting step is binding of *cis*-fluorophore from solution. We tested different concentrations of fluorophore in solution (5, 10, and 20 μM), which proportionately increases the binding rate. As can be seen with DFHBI-1T (left), adding higher concentrations of DFHBI-1T does not lead to an increased plateau of fluorescence. However, with DFNS, increasing concentrations of DFNS leads to an increased plateau of fluorescence. This suggests that binding of the *cis*-fluorophore in solution is the rate limiting step, not unbinding of *trans*-DFNS. Error bars indicate s.e.m. for $n=3$ cells per condition. The brightness was computed by measuring the signal in cells'

area and subtracting background based on the average signal of control cells. The plot for DFHBI-1T is taken from ref. 3.

Author Manuscript

Author Manuscript

Author Manuscript

Author Manuscript

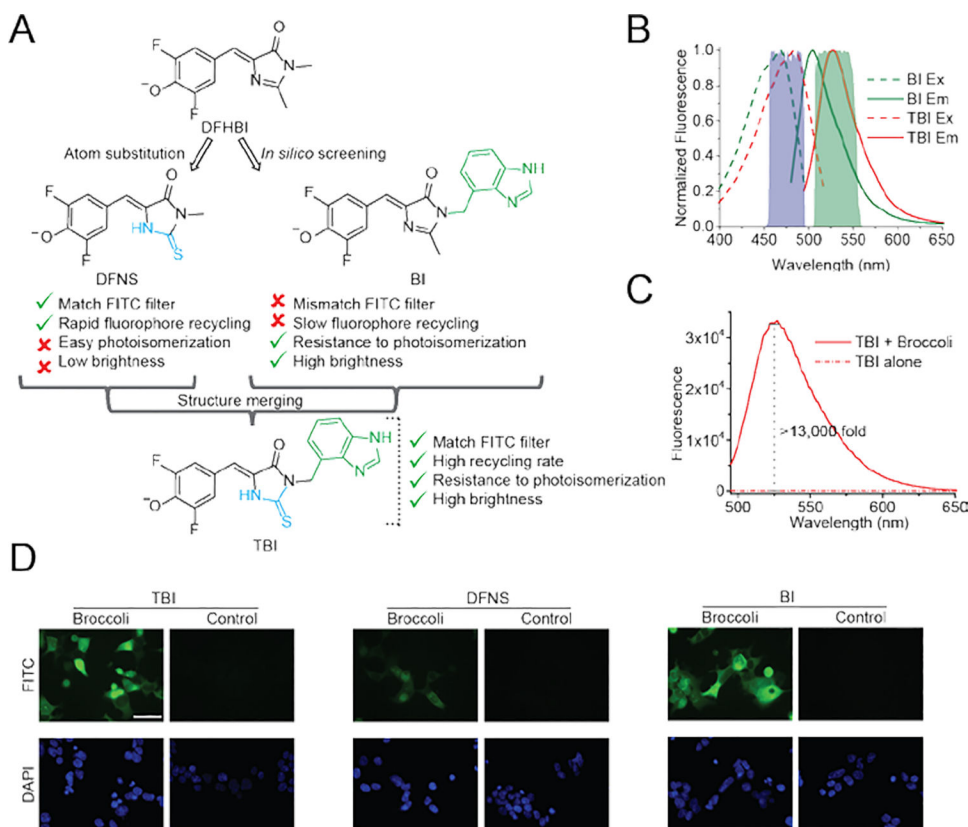


Figure 3. Design of TBI fluorophore based on BI and DFNS.

(A) To design a fluorophore with the desirable properties of both DFNS and BI, we structurally merged BI and DFNS. (B) The spectra of Broccoli-TBI is compatible with the commonly used FITC filter cube. Note that the emission of Broccoli-BI shows only partial overlap with the emission filter of the FITC filter cube, which will therefore reduce the total measured fluorescence output. Excitation (Ex, dotted line) and emission (Em, solid line) spectra were measured using 10 μM Broccoli and 0.5 μM TBI or BI in buffer containing 40 mM HEPES pH 7.4, 100 mM KCl and 1 mM MgCl_2 . (C) TBI exhibits low background and high fluorescence activation with Broccoli *in vitro*. Fluorescence emission spectra of TBI were obtained in the presence and absence of Broccoli. Spectra were measured in a solution containing 1 μM TBI, and either 0 or 10 μM Broccoli. (D) TBI retains high fluorescence of BI throughout the cytoplasm. HEK293T cells expressing circular Broccoli RNA were imaged in the presence of TBI, or DFNS or BI (10 μM). Images were acquired with a FITC filter cube for Broccoli fluorescence, and a DAPI filter cube for Hoechst 33342 staining. Exposure times: 100 ms for Broccoli, 10 ms for DAPI. Scale bar, 50 μm .

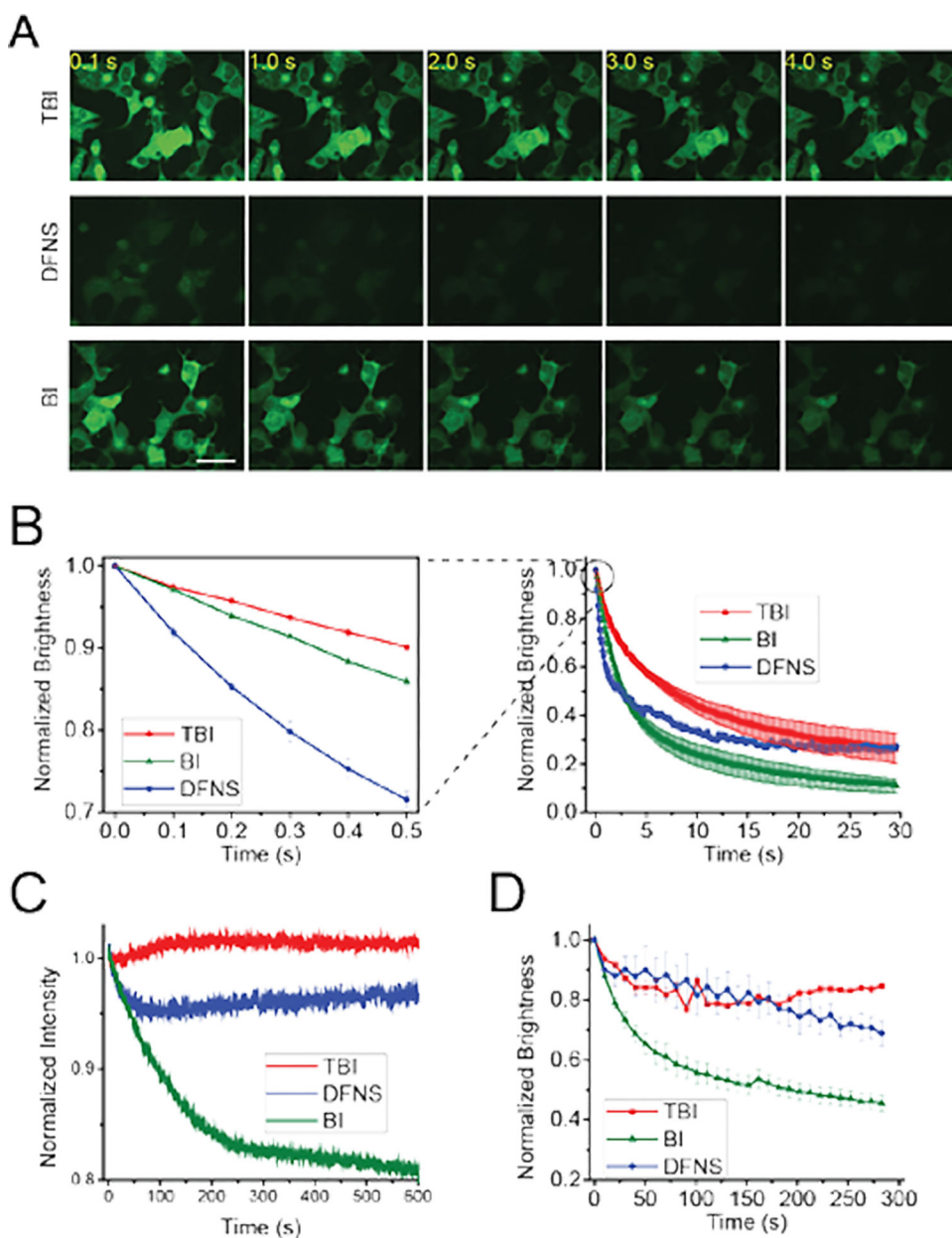
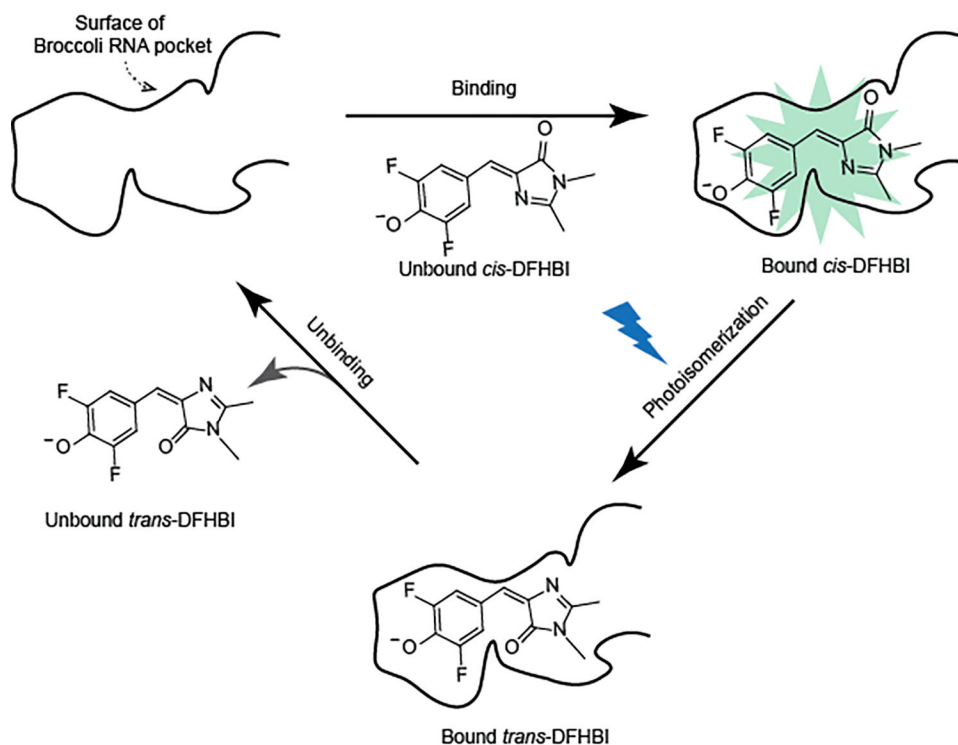


Figure 4. Broccoli-TBI exhibits high photostability and high fluorophore recycling rate. (A) and (B) TBI exhibits markedly improved photostability and a higher recycling rate compared to DFNS and BI in living cells. *In vivo* photostability of Broccoli-fluorophores (10 μ M) was assessed by continuous imaging of cells expressing circular Broccoli at an exposure time of 100 ms for each frame. Images were acquired using a 40 \times objective with a FITC filter cube for Broccoli fluorescence. Scale bar, 50 μ m. (B) Quantification of cellular fluorescence in panel (A). On the right is a time course over 30 s. The panel on the left shows the first 0.5 s in order to more easily detect the initial rate of fluorescence loss, which reflects the photoisomerization rate. As can be seen, TBI shows the least photoisomerization, and this rate is substantially improved relative to DFNS. To determine the fluorophore recycling rate, we examined the fluorescence plateau. As can be seen, both

TBI and DFNS exhibit a higher plateau compared to BI. Error bars indicate s.e.m. for n=3 cells per condition. Scale bar, 50 μm . (C) Broccoli-TBI exhibits high photostability *in vitro*. In these cuvette experiments measured in a fluorometer, we used solutions containing 0.1 μM fluorophore (TBI, DFNS, BI) and 1 μM Broccoli. (D) TBI exhibits a higher rebinding relative to BI. To determine the degree of rebinding, we examined the fluorescence recovery rate *in vivo*. *In vivo* brightness of Broccoli-fluorophores (10 μM) was measured every 10 s. Broccoli-expressing cells incubated with BI exhibited a drop in cellular fluorescence using this commonly used imaging protocol. However, cells incubated with TBI or DFNS exhibited a significantly smaller reduction in cellular fluorescence. Images were acquired with a FITC filter cube for Broccoli fluorescence. Error bars indicate s.e.m. for n=3 cells per condition. The plot for BI is taken from ref. 3.

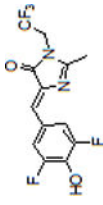
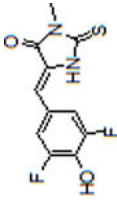
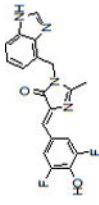
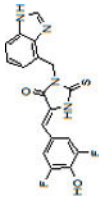


Scheme 1. The fluorescence output of the Broccoli-DFHBI complex is limited by photobleaching and a slow fluorophore recycling rate.

Schematic of the molecular steps that account for recycling process of Spinach/Broccoli and the resoration of fluorescence. Broccoli contains a pocket (indicated as a black solid curved line) that binds *cis*-DFHBI, which results in fluorescence. Photobleaching occurs by light-induced *cis-trans* photoisomerization of bound *cis*-DFHBI. *trans*-DFHBI then undergoes unbinding from the pocket. Lastly, *cis*-DFHBI from solution rebinds Broccoli, which results in restoration of fluorescence. Spinach/Broccoli bound to DFHBI exhibits slow recycling rate since *trans*-DFHBI undergoes slow unbinding from the pocket, and because *cis*-DFHBI binds Broccoli slowly.

Table 1.

Photophysical and Binding Properties of Fluorophore-Broccoli Complexes^a

Fluorophore	Excitation (nm)	Emission (nm)	Extinction Coefficient (M ⁻¹ , cm ⁻¹) ^b	Quantum Yield	Brightness ^c	K _d (nM)
DFHBI-IT alone 	428	500	35,400	0.00041	0.121	N/A
Broccoli-DFHBI-IT	470	505	28,900	0.41	100	305±39
DFNS alone 	435	527	37,700	0.00031	0.0974	N/A
Broccoli-DFNS	470	527	31,600	0.22	57.0	646±103
BI alone 	425	500	42,500	0.00048	0.171	N/A
Broccoli-BI	470	505	33,600	0.67	188	51±5
TBI alone 	433	524	43,300	0.00037	0.133	N/A
Broccoli-TBI	485	527	35,100	0.64	189	71±18

^aPhotophysical and binding properties of DFHBI-IT alone and Broccoli-DFHBI-IT, BI alone and Broccoli-BI are reported from a previous study.^[3] All data were measured at pH 7.4 at 25°C.

^bBrightness (extinction coefficient × quantum yield) is relative to Broccoli-DFHBI-IT.^[3]